March 2018

Hydrodynamic noise from a propeller in open sea condition

Marta CIANFERRA [a,1], Andrea PETRONIO [b] and Vincenzo ARMENIO [a]
[a] *Università degli Studi di Trieste, Dipartimento di Ingegneria e Architettura, via Alfonso Valerio 10, I-34127 Trieste, Italy*
[b] *Iefluids S.r.l., Piazzale Europa 1, I-34127 Trieste, Italy*

Abstract. In the present work a hybrid methodology is used to evaluate the hydrodynamic noise generated by a marine propeller in open sea condition. The hydrodynamic field is computed using Large Eddy simulation under the assumption of incompressible flow field; the acoustic field is reconstructed by applying the advective Ffowcs Williams and Hawkings equation. For the hydrodynamics, we use the dynamic Lagrangian model for the closure of the subgrid-scale stresses and a wall-layer model to skip the resolution of the viscous sub-layer. We consider a propeller well studied in literature for a single value of the advance ratio. A grid of about $6x10^6$ cells is used for reproducing accurately both the stresses over the propeller and the wake, the latter responsible of quadrupole noise. The equations are solved in a fixed-to-the-body frame of reference. The different noise generation mechanisms are investigated separately. Thickness and loading terms related to the propeller shape and velocity, provide significant pressure disturbance in the near field. The quadrupole noise component is obtained by integrating over an external permeable surface. Its contribution is investigated in relation to the presence of vortex persisting in the wake.

Keywords. hydrodynamic noise, LES, Ffowcs Williams and Hawkings, propeller, open water

1. Introduction

The study and evaluation of hydrodynamic noise is an interesting and growing field of investigation due to its own importance in several fields of application, including the marine propeller design. The latter may have a deep impact in terms of noise propagation in the sea environment affecting marine biosphere. In this regard, the regulation in protected sea regions is becoming more and more stringent, allowing for the transit only to certified "silent" ships [1]. The development of new generation noise prediction tools is thus required for the correct design of ship [2,3]. Nowadays, high-resolution unsteady and eddy-resolving numerical simulation of the turbulent field around a full-scale ship propeller is becoming computationally affordable as well as the turbulent noise prediction which is now at hand. In the present work we focus on the marine propeller, that it is one among the major sources of underwater noise. It generates noise according to two different mechanisms: the first one is associated with the propeller shape and rotational

[1] Corresponding Author: Marta Cianferra, E-mail: martacianferra@gmail.com.

velocity, generating pressure disturbances in the near field; the second one comes from turbulent coherent structures propagating downstream. Although the first effect has been well recognized in the past and evaluated through the use of simplified models, the second one has been usually neglected due to inherent difficulties in the evaluation of the wake from one side, and in the evaluation of the quadrupole terms representing the noise generated by the wake.

We use a hybrid methodology, meaning that we first evaluate the hydrodynamic field using a numerical technique, and then we evaluate the acoustic field using the Ffowcs Williams and Hawkings (FWH) equation. This methodology offers a number of advantages when compared to the direct solution of the compressible form of the Navier-Stokes equations (for details see [4] and literature therein cited).

The simulation of the hydrodynamic field is carried out solving the incompressible form of the filtered Navier-Stokes equations adopting Large Eddy simulation (LES). In LES, the large, energy-carrying structures are simulated directly through an unsteady 3D simulation, whereas the small and dissipative scales of turbulence are parametrized using a subgrid-scale model. The numerical results, in terms of instantaneous pressure and velocity fields, are then used to reconstruct the acoustic field by means of a post-processing tool that implements the advective form of the FWH equation. Although the resolved LES field does not contain the SGS contribution, recent literature has established that the unresolved field practically does not contribute to the composition of the overall radiated noise [5]. The evaluation of noise generated by a ship propeller, including the non-linear quadrupole part and using data coming from eddy resolving simulations, may be considered the state-of-art on this topic. Some recent work [6] proposed the use of the FWH porous formulation with RANS/DES data.

2. Numerical model

The problem under investigation is axial-symmetric, with a constant rotation rate. Under these conditions the governing equations can be recast in the rotating non-inertial frame of reference, thus adding the body forces accounting for rotational effects. The incompressible filtered Navier-Stokes equations are then formulated for the absolute velocity vector, as suggested in [8], with the Coriolis and centrifugal body-forces that take into account the rotational effects, along with the continuity equation:

$$\frac{\partial \overline{u}_i}{\partial t} + \frac{\partial}{\partial x_j}\left(\overline{u}_i\overline{u}_j - \overline{u}_i \varepsilon_{jkl}\omega_k x_l\right) = \frac{1}{\rho_0}\frac{\partial \overline{p}}{\partial x_i} - \varepsilon_{ijk}\omega_j\overline{u}_k + \nu\frac{\partial^2 \overline{u}_i}{\partial x_j \partial x_j} - \frac{\partial \tau_{ij}}{\partial x_j}, \tag{1}$$

$$\frac{\partial \overline{u}_i}{\partial x_i} = 0, \tag{2}$$

where the overbar denotes a filtered quantity. In eqs. 1,2 u_i denotes the fluid velocity along the x_i direction, t is time, ρ_0 and ν are respectively the fluid density and kinematic viscosity, p is the hydrodynamic pressure, ε_{ijk} is the Levi Civita III-order tensor, ω_i is the $i-$component of the rotation vector and τ_{ij} is the SGS stress tensor. Filtering is necessary in LES to separate the resolved fluctuating field from the unresolved one, whose effects are parametrized through the SGS model. Here we use a dynamic Smagorinsky model, with the constant averaged along the Lagrangian trajectory of the fluid particles [9]. For

details on the numerical model and SGS model, the reader is referred to [10] and to literature therein reported.

In order to simulate high-Reynolds number flows, the first grid point off the wall is placed within the inertial part of the boundary layer and the presence of the wall is accounted for through the use of a wall-layer model. We use an equilibrium wall stress model, in which the wall stress is obtained from instantaneous horizontal velocity at the first off-wall centroid based on law of the wall (details are in [11]).

2.1. Acoustic model

To reconstruct the acoustic field we adopt the advective FWH equation formulated in [4]. The non-linear terms of the equation, often regarded as quadrupole noise source terms, are evaluated by applying the porous formulation, meaning that the integrals are evaluated over a porous surface embedding the body and the entire wake. It reads as:

$$\begin{aligned} 4\pi \hat{p}_{2D}(\mathbf{x},t) = \quad & \frac{\partial}{\partial t}\int_{f=0}\left[(1-M_0\hat{r}_1)\frac{\rho_0 u_i \hat{n}_i}{r^*|1-M_r|}\right]_\tau dS - U_0\int_{f=0}\left[\frac{\rho_0 u_i \hat{n}_i \hat{r}_1^*}{r^{*2}|1-M_r|}\right]_\tau dS \\ & + \frac{1}{c_0}\frac{\partial}{\partial t}\int_{f=0}\left[\frac{L_{ij}\hat{n}_j\hat{r}_i}{r^*|1-M_r|}\right]_\tau dS + \int_{f=0}\left[\frac{L_{ij}\hat{n}_j\hat{r}_i^*}{r^{*2}|1-M_r|}\right]_\tau dS, \end{aligned} \tag{3}$$

where $\hat{n}$ is the (outward) unit normal vector to the surface element dS, $\hat{r}$ and $\hat{r}^*$ are unit radiation vectors (see [7] for more details), U_0 is the mean flow which advects the pressure acoustic field along the x-axis direction, r and r^* are the module of the radiation vectors $\mathbf{r}$ and $\mathbf{r}^*$ respectively, $M_0 = U_0/c_0$ is the inlet Mach number, M_r is the projection of the Mach vector along the source-observer direction and c_0 is the sound speed. The tensor L_{ij} appearing in (3) is given by

$$L_{ij} = [\rho_0 u_i \left(u_j + U_0\delta_{1j} - v_j\right) + P_{ij}],$$

where $P_{ij} = (p-p_0)\delta_{ij} - \sigma_{ij}$ is the compressive stress tensor, with $p-p_0$ the flow pressure perturbation with respect to the reference value p_0, σ_{ij} the viscous stress tensor and δ_{ij} the Kronecker delta.

Finally, t the observer time and τ the emission time. They are related by the compressibility delay equation:

$$\tau = t - \frac{|\mathbf{x}(t) - \mathbf{y}(\tau)|}{c_0}, \tag{4}$$

being $\mathbf{x}$ the observer position at the observer time t and $\mathbf{y}$ the source position at the corresponding emission time τ. If the control surface S coincides with the propeller surface, equation 3 gives thickness and loading noise terms, referred to as linear part of the equation. They represent the noise generated by the motion of the propeller and the pressure acting over the blades.

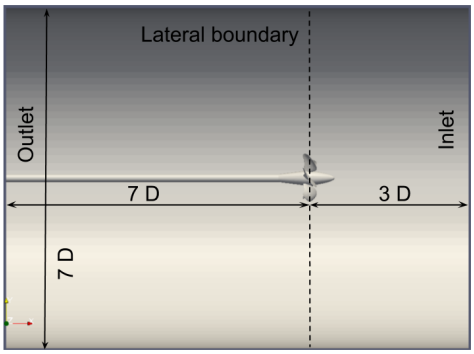

Figure 1. Schematic of the computational box used for the LES

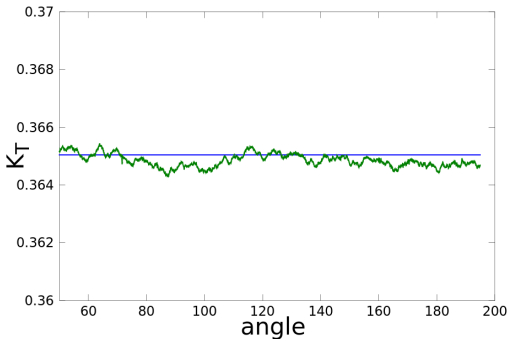

Figure 2. Time record of the K_T coefficient and mean value (straight line) obtained in the simulation

3. The analysis of the propeller

In this study we refer to a benchmark propeller, the SVA VP1304, designed for the smp workshops, in order to collect reliable experimental data. All the documentation, including the geometry, experimental data, numerical results from simulations, is available at https://www.sva-potsdam.de/en/potsdam-propeller-test-case-pptc, for both the uniform and non-uniform flow cases. The benchmark was introduced and discussed in the International Symposiums on Marine Propulsors of 2011 and 2015 respectively.

In the present study, we carry out the analysis of the propeller for a single value of the advance ratio

$$J_v = \frac{V_a}{nD} = 1.0683, \tag{5}$$

where V_a is the velocity along the direction of motion, n is the rotational velocity in revolutions per second (rps) and $D = 0.25\ m$ is the diameter of the propeller.

For the value of J_v herein considered, the values of the thrust (K_T) and torque (K_Q) coefficients are respectively:

$$K_T = \frac{T}{\rho n^2 D^4} = 0.3538, \qquad K_Q = \frac{Q}{\rho n^2 D^5} = 0.09096, \tag{6}$$

where T and Q are the thrust and the torque provided by the propeller. In the experimental set-up the rotation direction is right-handed.

The cylindrical numerical domain used for the LES is sketched in Fig. 1; it has a diameter of $7D$, and length of $10D$ as suggested in [8]. The blades plane is located $3D$ downstream the inlet and $7D$ upstream the outlet section. The grid is obtained in the following way: a cylindrical O-grid is created with streamwise cell clustering increasing close to the hub and the blades region, and with grid coarsening moving towards the lateral boundaries; the OpenFoam tool SnappyHexMesh is adopted to correctly reproduce the geometry. The mesh quality parameters fit the OpenFoam criteria. The total number of cells is around 4 millions for a preliminary mesh, and about 6 millions for the final mesh in which the wake region is refined in order to reproduce adequately the tip-vortex as well as the wake features. At the blades, both meshes have an uniform value of the first grid point off-the-wall $y_1^+ \sim 13.6$, achieved without the need of using prismatic layers ($y_1^+ = y_1/(\nu/u_\tau)$ where $u_\tau = \sqrt{\tau_w/\rho_0}$ with τ_w the mean shear stress).

3.1. Initial and boundary Conditions

A uniform flow field with mean velocity $V_a = 4\ m/s$ is imposed at the inlet, slip condition is given at lateral boundaries and zero gradient condition is enforced at the outlet. At the solid walls of the shaft, hub and blades, the tangential velocity is imposed based on $u_t(r) = \Omega \times r$, with r distance from the rotation axis, and $\Omega = 2\,\pi n$, with $n = 15\ rps$. The LES is started from a solution obtained with a RANS model in order to avoid the initial transitional development phase.

3.2. Fluid-dynamic analysis

The simulation results are compared with the experimental data. The numerically computed force and torque over the five blades give coefficients $K_{T_s} = 0.3650$, $K_{Q_s} = 0.09277$ corresponding to errors of $e_{K_T} = 3.18\%$ and $e_{K_Q} = 1.89\%$ respectively.

The signal in time of the K_{T_s} is shown in figure 2, over the period of time between 50 and 200 degrees of rotation. Also, the figure reports the value of K_T averaged in time.

The errors may be considered not marginal but in any case they are aligned with other numerical simulation relying on wall-functions for similar case. Moreover, the mesh we are testing does not have any prismatic layer, and the mesh at the blades is not optimal in this sense. Also, the simulation time was not long enough to obtain convergent statistics. However we stress out that these results are encouraging still being preliminary. We can assume that such a fluid dynamic field is acceptable for carrying out the acoustic analysis.

In figure 3 we show the tip-vortex structures in the wake of the blades highlighted by means of the λ_2 method.The typical helical structures is well present, each one starting at the tip of a blade. Also, turbulent wake is present although not evidenced in the figure.

3.3. Acoustic analysis

In this section results obtained using the the advective FW-H porous formulation are discussed. The control (porous) surface S was chosen as depicted in figure 4, namely a

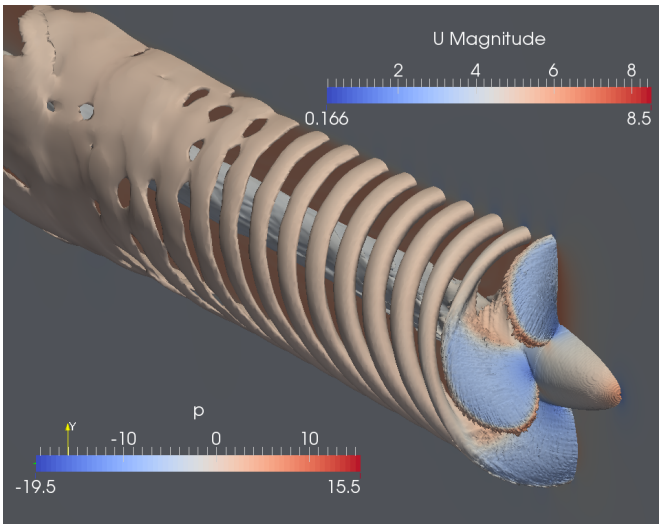

Figure 3. Visualization of the tip-vortex coherent structures through the λ_2 method.

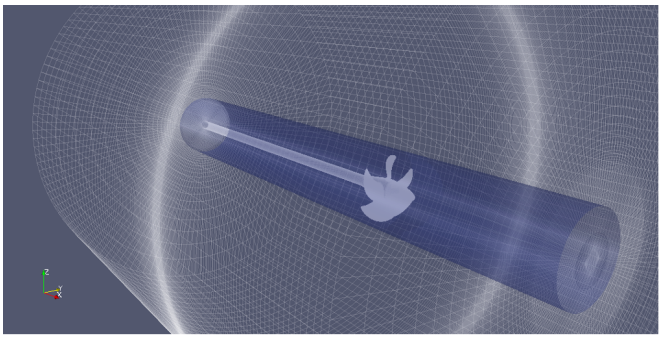

Figure 4. Sketch of the control surface adopted for FW-H porous domain, blue cylinder of radius $1.4m$.

cylindrical surface of radius $1.4m$, whose axis corresponds to the propeller axis. Since the frame of reference is assumed to rotate together with the propeller, the velocity of the porous domain v needs to be considered.

Three different microphones are considered, respectively located at $1.33R$ (mic 1), $13.3R$ (mic 2) and $133R$ (mic 3) from the axis of symmetry, on the plane of the propeller $x = 0$. Results are in figure 5, showing the Sound Spectrum Level evaluated as $SPL = 20\log_{10}(A/p_{ref})$, being A the amplitude of the signal and $p_{ref} = 1\mu Pa$ the reference pressure for underwater measurements. The signal is strongly periodic with a frequency equal to nN, being n number of revolutions per second and N the number of blades. This periodicity is evidenced by the peaks in the spectra at a frequency of about 88 Hz. The peak is high close to the propeller and it decreases in amplitude moving in the far field, being still present at the farther microphone. Apart the peak, a noise signature spread over a wide frequency range is present, highlighting the inherent non linear nature of the phenomenon. In the region close to the propeller, the noise peak is of the order of 115 decibels, in agreement with the literature data for this class of problem.

To investigate on non-linear effects, a fourth microphone was considered (mic 4) at distance $1.33R$ from the axis of symmetry and $x = 3R$, downstream. The results (not depicted) show that the porous formulation is able to detect a secondary higher frequency associated to wake effects, the latter non detectable by the linear term. Also, at the position of mic 4, the peak of noise given by the linear part (loading and thickness noise terms) is of the order of 85 decibels, whereas the additional contribution of the wake (non-linear or quadrupole term) is of about 10 decibels over a wide frequency range.

A consideration on the importance of time delay computation (see eq. (4)) can be addressed by calculating the retarded surface Σ, where the linear terms are evaluated. The procedure of calculating Σ consists of:

- set a time t^* of acoustic signal reception;
- calculate τ with the bisection method on the function $f(\tau) = t^* - \tau - |\mathbf{x} - \mathbf{y}(\tau)|/c_0$ where $\mathbf{y}(\tau)$ are the points on the propeller that are rotating and $\mathbf{x}$ is a microphone location;
- once τ^* is found that satisfies $f(\tau^*) = 0$, we calculate $\mathbf{y}(\tau^*)$ that corresponds to the retarded surface.

The main result is that at very low rotational Mach numbers, as the one considered in this study, the retarded surface practically coincides with the solid propeller surface, see figure 6. It means that no significant time shift between pressure signals from different source points is occurring, and that direct integration of kernels is allowed. This becomes significant in case the direct volume integration of quadrupole terms is performed (see [4] for a discussion). This is the topic of successive research.

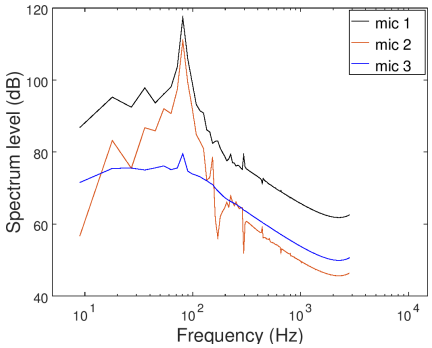

Figure 5. Sound Spectrum Level obtained with FW-H porous equation. The three measurement points are at $x = 0$ and at a distance: $1.33R$ (mic1), $13.3R$ (mic2) and $133R$ (mic3) from the axis of rotation.

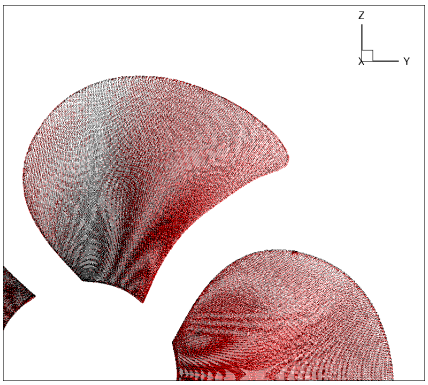

Figure 6. Retarded surface Σ (red) and propeller surface (black). Note that they are practically overlapped.

4. Conclusions

In the present paper the acoustic signature of a ship propeller in open sea condition is investigated. We use the hybrid methodology, where the solution of the fluid dynamic field is decoupled from that of the acoustic field. Further, in order to reproduce realistically the wake of the propeller as well as the pressure distribution around it, a large eddy simu-

lation has been carried out with a dynamic Lagrangian Smagorisky model. The acoustic field has been computed solving the advective FW-H equation by using the porous formulation. The results of the simulation give acceptable prediction of the propeller coefficients (within few percentages), aligned with other numerical simulation. The acoustic solver reproduces an accurate noise spectrum, both in frequency and in level. Also, the present preliminary analysis shows that the wake contributes for about 15% of the total radiated noise over the entire frequency spectrum. A more detailed analysis in underway and is the topic of a successive publication.

Acknowledgements

This work was supported by Region FVG-POR FESR 2014-2020, Fondo Europeo di Sviluppo Regionale, Project PRELICA "Metodologie avanzate per la progettazione idroacustica dell'elica navale. We also thank Dr. Federico Roman, Iefluids s.r.l., for his technical assistance, his precious comments and suggestions during the development of the presented work.

References

[1] DNV. Rules for Classification of Ships, Part 6 Chapter 24. SILENT CLASS NOTATION, JANUARY 2010.

[2] Mahesh K., Kumarc P., Gnanaskandan A. and Nitzkorski Z., *LES Applied to Ship Research*, Journal of Ship Research, Vol. 59, No. 4, (2015), 238245.

[3] Ianniello S., Muscari R. and Di Mascio A., *Ship underwater noise assessment by the acoustic analogy, part III: measurements versus numerical predictions on a full-scale ship*, J Mar Sci Technol, (2013).

[4] M. Cianferra, V. Armenio and S. Ianniello, Hydroacoustic noise from different geometries, *International Journal Heat Fluid Flow*, (Available online 22 December 2017), In Press.

[5] U. Piomelli, L.S. Craig and S. Sarkar, On the computation of sound by large-eddy simulation. *Journal of Engineering Mathematics* **32** (1997), 217–236.

[6] Ianniello S., Muscari R. and Di Mascio A., *Ship underwater noise assessment by the acoustic analogy. Part I: nonlinear analysis of a marine propeller in a uniform flow*, J Mar Sci Technol, (2013).

[7] Najafi-Yazdi A., Bres G. A. and Mongeau L., *An acoustic analogy formulation for moving sources in uniformly moving media*, Proceedings of Royal Society London, A467, (2011), 144-165.

[8] P. Kumar, K. Mahesh: Large eddy simulation of propeller wake instabilities, *Journal of Fluid Mechanics* **814** (2017), 361–396.

[9] C. Meneveau, T.S. Lund, W. H. Cabot, A Lagrangian dynamic subgrid-scale model of turbulence, *Journal of Fluid Mechanics* **319** (1996), 353–385.

[10] C. Cintolesi, A. Petronio, V. Armenio, Large eddy simulation of turbulent buoyant flow in a confined cavity with conjugate heat transfer, *Physics of Fluids* **27** (2015), 095109.

[11] A. Fakhari, C. Cintolesi, A. Petronio, F. Roman and V. Armenio, Numerical simulation of hot smoke plumes from funnels, *submitted to NAV 2018, 19th International Conference on Ship & Maritime Research* (2018).

[12] C. Cintolesi, A. Petronio and V. Armenio, Large-eddy simulation of thin film evaporation and condensation from a hot plate in enclosure: first order statistics, *International Journal of Heat Mass Transfer* **1001** (2016), 1123–1137.